



HAL
open science

Intralamellar structural modifications related to the proton exchanging in KNbO layered phase

M.A. Bizeto, F. Leroux, A.L. Shiguihara, M.L.A. Temperini, O. Sala, V.R.L. Constantino

► **To cite this version:**

M.A. Bizeto, F. Leroux, A.L. Shiguihara, M.L.A. Temperini, O. Sala, et al.. Intralamellar structural modifications related to the proton exchanging in KNbO layered phase. *Journal of Physics and Chemistry of Solids*, 2010, 71 (4), pp.560. 10.1016/j.jpcs.2009.12.036 . hal-00628280

HAL Id: hal-00628280

<https://hal.science/hal-00628280>

Submitted on 1 Oct 2011

HAL is a multi-disciplinary open access archive for the deposit and dissemination of scientific research documents, whether they are published or not. The documents may come from teaching and research institutions in France or abroad, or from public or private research centers.

L'archive ouverte pluridisciplinaire **HAL**, est destinée au dépôt et à la diffusion de documents scientifiques de niveau recherche, publiés ou non, émanant des établissements d'enseignement et de recherche français ou étrangers, des laboratoires publics ou privés.

Author's Accepted Manuscript

Intralamellar structural modifications related to the proton exchanging in $K_4Nb_6O_{17}$ layered phase

M.A. Bizeto, F. Leroux, A.L. Shiguihara, M.L.A. Temperini, O. Sala, V.R.L. Constantino

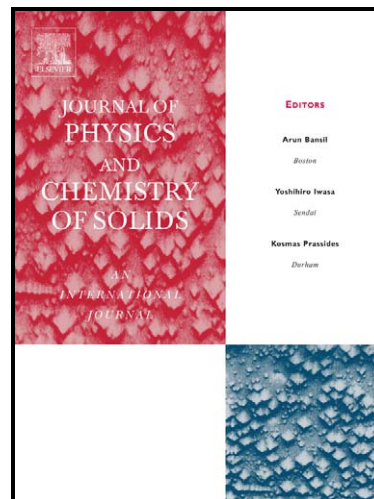
PII: S0022-3697(09)00378-3
DOI: doi:10.1016/j.jpics.2009.12.036
Reference: PCS 6024

To appear in: *Journal of Physics and Chemistry of Solids*

Received date: 10 May 2009
Accepted date: 10 June 2009

Cite this article as: M.A. Bizeto, F. Leroux, A.L. Shiguihara, M.L.A. Temperini, O. Sala and V.R.L. Constantino, Intralamellar structural modifications related to the proton exchanging in $K_4Nb_6O_{17}$ layered phase, *Journal of Physics and Chemistry of Solids*, doi:10.1016/j.jpics.2009.12.036

This is a PDF file of an unedited manuscript that has been accepted for publication. As a service to our customers we are providing this early version of the manuscript. The manuscript will undergo copyediting, typesetting, and review of the resulting galley proof before it is published in its final citable form. Please note that during the production process errors may be discovered which could affect the content, and all legal disclaimers that apply to the journal pertain.



www.elsevier.com/locate/jpics



Intralamellar structural modifications related to the proton exchanging in $K_4Nb_6O_{17}$ layered phase

M. A. Bizeto^a, F. Leroux^{b*}, A. L. Shiguihara^c, M. L. A. Temperini^c, O. Sala^c, V. R. L. Constantino^{c*}

^a Departamento de Ciências Exatas e da Terra, Universidade Federal de São Paulo - Campus Diadema, Rua Prof. Artur Riedel, 275, CEP 09972-270, Diadema - SP, Brazil.

^b Laboratoire des Matériaux Inorganiques, UMR 6002-CNRS, Université Blaise Pascal, 24 av. des Landais, 63177 Aubière cedex, France.

^c Instituto de Química, Universidade de São Paulo, Av. Prof. Lineu Prestes 748, CEP 05508-000, São Paulo - SP, Brazil.

ABSTRACT

Basic structural aspects about the layered hexaniobate of $K_4Nb_6O_{17}$ composition and its proton-exchanged form were investigated mainly by spectroscopic techniques. Raman spectra of hydrous $K_4Nb_6O_{17}$ and $H_2K_2Nb_6O_{17} \cdot H_2O$ show significant modifications in the 950-800 cm^{-1} region (Nb-O stretching mode of highly distorted NbO_6 octahedra). The band at 900 cm^{-1} shifts to 940 cm^{-1} after the replacement of K^+ ion by proton. Raman spectra of the original materials and the related deuterated samples are similar suggesting that no isotopic effect occurs. Major modifications were observed when $H_2K_2Nb_6O_{17}$ was dehydrated: the relative intensity of the band at 940 cm^{-1} decreases and new bands seems to be present at about 860-890 cm^{-1} . The H^+ ions should be shielded by the hydration sphere what preclude the interaction with the layers. Removing the water molecules, H^+ ions can establish a strong interaction with oxygen atoms, decreasing the bond order of Nb-O linkage. X-ray absorption near edge structure studies performed at Nb K-edge indicate that the niobium coordination number and oxidation state remain identical after the replacement of potassium by proton. From the refinement of the fine structure, it appears that the Nb-Nb coordination shell is divided into two main contributions of about 0.33 and 0.39 nm, and interestingly the population, *i.e.*, the number of backscattering atoms is inverted between the two hexaniobate materials.

Keywords: A. Inorganic compounds; B. Raman spectroscopy; C. X-ray absorption spectroscopy

Article history

Received: May 10, 2009

Accepted: Jun. 10, 2009

1. Introduction

Layered niobates are an emerging class of solid state precursors for nanostructured materials preparation due to their semiconductor, structural and optical properties, which

*Corresponding author. Tel.: +33473407036; fax: +33473407108.

E-mail address: fabrice.leroux@univ-bpclermont.fr

permit the assembling of new and interesting materials for different purposes [1]. The main studied layered niobate phase is the metal alkaline hexaniobate whose structure was detailed for $Rb_4Nb_6O_{17}$ [2,3], $K_4Nb_6O_{17}$ [3] and $Cs_4Nb_6O_{17}$ [3]. All these niobate phases are isostructural and have negative charged slabs constituted of double chains of corner and edge shared $[NbO_6]$ octahedral units in which one octahedron unit out of two is periodically missing in the second chain (Fig. 1). The alkali metal ion occupies the interlayer region [3].

$K_4Nb_6O_{17}$ is the most common precursor in the hexaniobate works and its unit cell contains four layers along the *b*-axis and two types of interlayer regions, denoted by I and II [3]. These interlayer regions are structurally and reactively distinct. Only interlayer I can be hydrated, producing the trihydrate and pentahydrate forms. In Fig. 1 are indicated the K^+ -O interactions that are maintained or broken after water molecules intercalation between the layers. The interlayer reactivity of the hexaniobate is also dependent on the interlayer cation. To transform $K_4Nb_6O_{17}$ into a precursor more able to undergo further chemical and structural modifications, the potassium ions are usually exchanged by protons (H^+). As it was previously reported [4], when this reaction is carried out under mild conditions, it is produced an ordered interstratified lamellar material of $H_2K_2Nb_6O_{17} \cdot H_2O$ composition, where only the potassium ions located at interlayer I are exchanged.

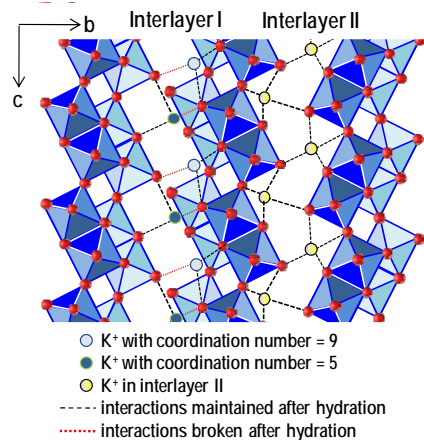


Fig. 1. Representation of $K_4Nb_6O_{17}$ structure in the anhydrous phase; (---) bonds maintained after the water intercalation; (••••) broken bonds in the hydration process.

The proton-exchanged hexaniobate has a fundamental participation in the production of nanosheets and nanoscrolls through exfoliation reactions [5] and, consequently, a significant importance to the development of new materials using the niobate anisotropic particles as nanobuilding blocks. The colloidal nanosheets can be assembled into nanostructured devices for photocurrent or photoluminescence generation [6], polymer nanocomposites [7], macroporous solids [8], catalysts for oxidation reaction [9], hybrids materials containing natural dyes [10] and systems for H_2 photo-production [11].

A finely structural characterization of the hexaniobate precursors can assist to better understand the properties and modifications that are related to the particles morphological transformation after ion-exchange, exfoliation and curling processes. In order to contribute to the niobate studies, basic structural aspects related to the potassium and the proton-exchanged hexaniobate were investigated through spectroscopic techniques sensitive to the short-range structure.

Raman spectroscopy, a technique responsive to structure and bond order modifications, has been used to characterize niobate oxides such as the layered phases [12]. However the interpretation of shifts in the Nb-O stretching region when K^+ is replaced by H^+ in layered niobates is an open question in the literature [12,13]. In this work, the Raman spectra of the potassium (sample I) and acidic (sample II) hexaniobate were analyzed after the contact of the anhydrous samples with deuterated water and also after heating for the interlayer water molecules release.

In a next step, X-ray absorption spectroscopy (XAS) was used to scrutinize the local arrangement around Nb atoms. XAS is known to unravel local arrangement even for material presenting unusual morphology, such as exfoliated MoS_2

layers [14] or titanate nanotubes/nanobelts [15]. X-ray absorption near edge structure spectroscopy (XANES) data of both samples I and II were analyzed at the niobium K-edge and compared to $H-Nb_2O_5$. The extended X-ray absorption fine structure (EXAFS) oscillations were refined, and the local order around the niobium atoms is discussed.

2. Experimental

2.1 Preparation of the samples

$K_4Nb_6O_{17}$ was prepared by ceramic method heating a stoichiometric mixture of Nb_2O_5 (Companhia Brasileira de Metalurgia e Mineração, CBMM, Brazil) and K_2CO_3 (Merck) at $1100^\circ C$ for 10h, as previously described [9,10]. The heating process was made in two steps of 5 h each with one grinding between them. Crystal structure of hydrous $K_4Nb_6O_{17}$ was confirmed by powder X-ray diffractometry ($d_{040} = 0.94$ nm). The acidic form was prepared by ion exchange, refluxing a suspension of $K_4Nb_6O_{17}$ in a 6 mol/L HNO_3 solution for 5 days under heating at about $60^\circ C$. The acid solution was replaced after 3 days. The solid was centrifuged, washed with deionized water and dried in a desiccator with silica-gel under vacuum. Powder X-ray diffractometry and thermogravimetric analysis (TG) confirmed the isolation of the acidic hexaniobate of $H_2K_2Nb_6O_{17} \cdot H_2O$ composition ($d_{040} = 0.80$ nm), as previously reported [4].

Aiming the preparation of samples containing deuterated water, the two hydrous hexaniobate samples were dehydrated under N_2 flow of 50 mL/min, in a thermogravimetric equipment, using an alumina crucible and heating rate of $10^\circ C/min$. Hydrous $K_4Nb_6O_{17}$ (sample I) was calcined at $400^\circ C$ for 30 min while $H_2K_2Nb_6O_{17} \cdot H_2O$ (sample II) was heated up to $250^\circ C$ and kept at this temperature for 30 min. After the furnace temperature reached the room temperature, the equipment was open and the samples were immediately added to recipients containing deuterated water (Aldrich). The recipients were maintained closed to avoid the contact with atmospheric water vapor.

2.2 Techniques of Characterization

XRD patterns of powdered samples were recorded on a Rigaku diffractometer model Miniflex using $Cu-K\alpha$ radiation (1.541 \AA , 30 kV and 15 mA). Mass coupled thermogravimetric analyses (TG-MS) were recorded on a Netzsch thermoanalyser model TGA/DSC 490 PC Luxx coupled to an Aëolos 403C mass-spectrometer.

Raman spectra were obtained in a Jobin Yvon U1000 spectrometer equipped with a Hamamatsu model C4877-01 phototube. The laser line used was the 514.5 nm from Coherent Innova 90 Kr⁺ having 50 mW at the sample. The spectral slit was 6 cm^{-1} .

X-ray absorption spectroscopy XAS studies were performed at LNLS (Brazilian Synchrotron Light Laboratory, Campinas, Brazil) using X-ray synchrotron radiation (1.37 GeV positrons, average intensity of 175 mA) at the DO4B-XAS1 beam line. Data were collected at room temperature in transmission mode at Nb K-edge, $18985.6 \pm 0.4 \text{ eV}$. For the extended X-ray absorption fine structure, a Si (220) crystal monochromator scanned the energy in 2 eV-steps from 18900 to 18980 eV (accumulation time of 1 s was used per point), 0.5 eV-steps from 18980 to 19060 eV (1 s), 2 eV-steps from 19060 to 19200 eV (1 s), 2 eV-steps from 19200 to 20100 (2 s). Five spectra were recorded for each sample.

Extraction and analysis of EXAFS data was performed following standard procedures as reported elsewhere [14]. The $\chi(k)$ signal was fitted by using the classical plane-wave single scattering approximation: $\chi(k) = S_0^2 \sum A_i(k) \cdot \sin[2k \cdot r_i + \phi_i(k)]$,

with $A_i(k)$ amplitude equal to $(N_i/k_i r_i^3) \cdot F_i(k) \cdot \exp(-2k^2 \sigma_i^2) \cdot \exp(-2r_i/\Gamma)$, where r_i is the interatomic distance, ϕ_i the total phase shift of the i^{th} shell, N_i the effective coordination number, σ_i the Debye-Waller factor, $F_i(k)$ the backscattering amplitude and Γ the free-mean path. To estimate the relative part of the cations contributing to the metal-metal correlation, the number of backscattering atoms was free to move during the refinement. This guarantees all possible cation ratios for the second shell. $H\text{-Nb}_2\text{O}_5$ was taken as reference compound [16]. All results were refined using FEFF 8 for MAC.

3. Results and Discussion

The vibrational spectra of hexaniobate are dominated by bands attributed to internal vibrational modes of distorted NbO_6 octahedra (linked by corner and by edge sharing) in the 200-1000 cm^{-1} region and also by external vibrations of the crystal below 170 cm^{-1} [12,17]. Fig. 2 shows that Raman spectra between both hexaniobates **I** and **II** exhibit significant modifications in the following regions: 950-800 cm^{-1} (Nb-O terminal stretching mode of highly distorted NbO_6 octahedra), 700-500 cm^{-1} (Nb-O stretching of slightly distorted octahedra) and 300-200 cm^{-1} (bending modes of the Nb-O-Nb linkages).

The band at 900 cm^{-1} assigned to short Nb-O bonds shifts to 940 cm^{-1} after the replacement of K^+ by H^+ ions, as it was observed in other works [13,18]. This band also shows a shift for the high wavenumber region when the layered niobate oxides of composition KNb_3O_8 and $\text{KCaNb}_3\text{O}_{10}$ are protonated [12,13]. It is expected that the interaction between proton ions and the oxygen atoms of NbO_6 units decreases the metal-oxygen bond order, bringing about the shift of $\nu\text{Nb-O}$ to the low wavenumber region. However, the opposite shifting is observed. Fig. 2 also shows spectral modifications in the 700-500 cm^{-1} region. The set of bands assigned to the $\nu\text{Nb-O}$ of slightly distorted octahedral also is moved to high energy region after the proton-exchange reaction.

In order to understand whether the spectral modifications are related to hydrogen species (such as hydronium ion, H_3O^+) introduced in the hexaniobate, the pristine and the proton-exchanged materials were deuterated after dehydration and posterior contact with liquid D_2O , as described in the experimental section. TG curves show that anhydrous hexaniobate materials are obtained after heat $\text{K}_4\text{Nb}_6\text{O}_{17}$ and $\text{H}_2\text{K}_2\text{Nb}_6\text{O}_{17}$ up to about 330°C and 250°C, respectively, as previously reported [4,19]. TG-MS data confirmed the insertion of deuterated species into the interlayer region since it was detected fragments with $m/z = 18, 19$ and 20 u in the gas phase related to the weight loss events.

Raman spectra of hydrated and deuterated $\text{K}_4\text{Nb}_6\text{O}_{17}$ are similar (Figure 2). There are not alterations in the bands positions; the presence of heavy water promotes a better resolution of the bands in the 700-500 cm^{-1} region compared to the pristine material. Similar results were obtained analyzing the vibrational spectra of hydrated and deuterated $\text{H}_2\text{K}_2\text{Nb}_6\text{O}_{17}$ (Fig. 2). Hence, the lack of significant modifications in the bands wavenumber and also of new bands point out that no isotopic effect occurs and that the appearance of the band at 940 cm^{-1} in the acidic hexaniobate is not related to hydrogen species.

In the next step, the potassium (sample **I**) and the proton-exchanged (sample **II**) hexaniobate were dehydrated in order to evaluate the water role in their structures. Considering the $\text{K}_4\text{Nb}_6\text{O}_{17}$ spectra before and after calcination at 500°C (Fig. 3), any important shift can be observed. As it can be seen in Fig. 1, the water release establishes the interaction between K^+ ions and some oxygen atoms of the layers surface that can contribute to a better resolution of the bands when compared to the original hydrous material.

On the other hand, in the Raman spectrum of the acidic hexaniobate (Fig. 3), the water liberation carries out a great spectral variation in the Nb-O stretching region: the decrease

of relative intensity of the band at 940 cm^{-1} and the presence of new bands at about 860 and 890 cm^{-1} . The structure of hexaniobate interlayer region occupied by H^+ is unknown (no crystallographic data are reported), but it is possible to suppose that the cations interact with water molecules and with the oxygen atoms of the niobium octahedra that compose the layers. The enthalpy of hydration of H^+ is -1090 kJ/mol while for potassium cation is -352 kJ/mol [20]. Hence, $\text{H}_2\text{K}_2\text{Nb}_6\text{O}_{17}$ sample is much more sensitive to dehydration than the potassium hexaniobate. It is possible to infer that in the proton-exchanged hexaniobate the cation interaction with water molecules is much stronger than the H^+ interaction with the NbO_6 layer units. In the hydrous $\text{K}_4\text{Nb}_6\text{O}_{17}$, the interaction $\text{Nb-O} \cdots \text{K}^+$ is more effective than the interaction $\text{K}^+ \cdots \text{OH}_2$. Hence the K^+ replacement by H^+ provokes an increase in the bond order of Nb-O and, consequently, a shift of the band related to $\nu\text{Nb-O}$ to high wavenumber. The H^+ ions should be shielded by the hydration sphere what preclude the interaction with the layers. Removing the water molecules by heating, H^+ ions can establish a strong interaction with the oxygen atoms of the layers. This assumption could explain the intensity decrease of the band at 940 cm^{-1} ($\nu\text{Nb-O}$) and the presence of new bands at lower wavenumber (Fig. 3).

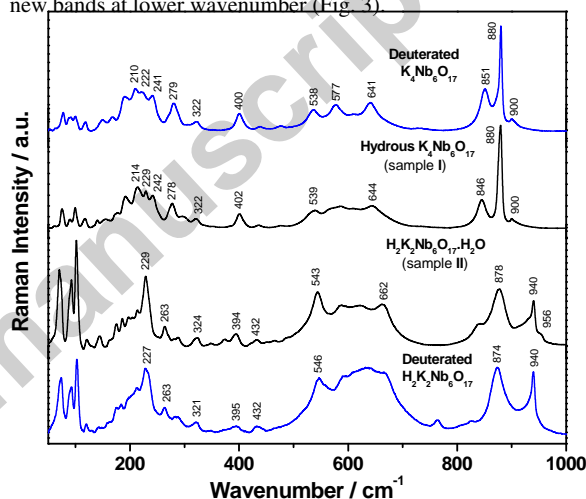


Fig. 2. Raman spectra of hydrous $\text{K}_4\text{Nb}_6\text{O}_{17}$ (sample **I**), $\text{H}_2\text{K}_2\text{Nb}_6\text{O}_{17} \cdot \text{H}_2\text{O}$ (sample **II**) and their deuterated forms prepared as described in the experimental section.

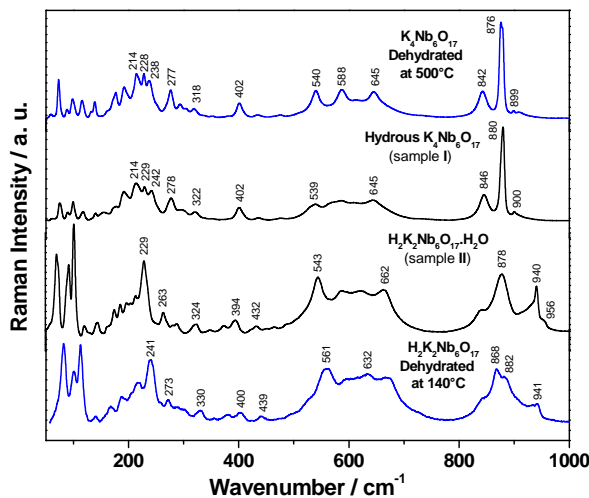


Fig. 3. Raman spectra of hydrous $K_4Nb_6O_{17}$ (sample **I**), $H_2K_2Nb_6O_{17} \cdot H_2O$ (sample **II**) and after dehydration by heating treatment.

As mentioned above, the vibrational bands arising in the 300-200 cm^{-1} region are attributed to bending modes of the Nb-O-Nb linkages and the observed differences between samples **I** and **II** may be interpreted some modifications (corrugation) arising in the NbO_6 chains when K^+ ions are exchanged by proton. Such modifications in the hexaniobate layer plane (*ac* plane) cannot be detected by XRD technique since the related diffraction plans (200) and (002) are similar between $K_4Nb_6O_{17}$ and $H_2K_2Nb_6O_{17}$. In order to shed some direct lights on the local order, XAS technique was here employed.

XANES intensity profile between $H-Nb_2O_5$ and both samples **I** and **II** is superimposable (supplementary), suggesting that the octahedral cage NbO_6 is similar in the compounds. Fourier transforms modulus (also called pseudo-radial distribution PRD) of the EXAFS oscillations at Nb K-edge for hydrous $K_4Nb_6O_{17}$ and $H_2K_2Nb_6O_{17} \cdot H_2O$ are displayed in Fig.4. They present features characteristic of a $H-Nb_2O_5$ -type phase. Refinement of $H-Nb_2O_5$ reference was carried out by averaging the crystallographic data (Table 1 and supplementary).

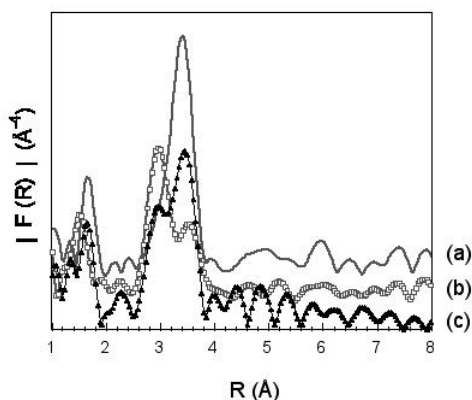


Fig. 4. Moduli of the Fourier transform for (a) $H-Nb_2O_5$, and samples (b) **I** and (c) **II**. The distances are not corrected from phase shifts.

Table 1. XAS fit results and crystallographic data for reference samples^a according to [16]

Sample	Atom	N	R (Å)	σ^2 (10^{-3}Å^2)	ρ^a (%)
$H-Nb_2O_5^b$	O	5.93	2.00	2.5	2
	Nb	1.07	3.39	3.4	
	Nb	3.50	3.83	3.3	
II	O	6.0	2.0	2.6	1.5
	Nb	2.47	3.32	4.5	
	Nb	3.11	3.87	3.9	
I	O	6.0	1.99	2.6	2
	Nb	3.17	3.30	4.2	
	Nb	2.95	3.94	4.1	

^a The residual ρ factor is defined as $\rho = [\sum(k^3 \chi_{exp}(k) - k^3 \chi_{theo}(k))^2 / \sum(k^3 \chi_{exp}(k))^2]^{1/2}$. The commonly accepted fitting accuracy is of about 0.02 Å for the distance and 15 to 20% for the number of neighbors.

^b From structural data: $H-Nb_2O_5$ phase crystallizes in space group P2/m with a monoclinic symmetry, lattice parameters of $a = 21.153$, $b = 3.823$ and $c = 19.356$ Å, $\beta = 119.80^\circ$, $Z=14$. Distances in $H-Nb_2O_5$ phase: 15 Nb sites, all of them octahedron except for one tetrahedrally coordinated Nb1 on (2i) 0, $\pm y, 0$. First distances Nb-O = 4 at 1.825,

then 6 at 1.968, 2.005, 2.006, 1.998, 2.050, 1.987, 2.034, 2.004, 1.992, 1.998, 2.018, 1.999, 1.999, and 1.972 Å. The site multiplicity is 2 except for Nb1 and Nb2 and equal to 1. Average distance $\langle Nb-O \rangle$ is then 5.93 oxygen atoms at 1.999 Å, taken as 2.00 Å in the EXAFS refinements. Nearest average contribution $\langle Nb-Nb \rangle$ on 128 distances gives 1.07 Nb at 3.395 Å and 3.5 Nb at 3.827 Å.

The similarities between both samples **I**, **II** and $H-Nb_2O_5$ PRD indicate that the main feature characteristic of the niobate framework is preserved, however it does not discard some slight change in the local Nb-surrounding. Indeed, the refinement of the coordination shell Nb-O gives rise to a distance closely related to the average Nb-O distance into $H-Nb_2O_5$ phase (Table 1) but there are slight changes in the Nb-Nb atoms vicinity. The quality of the refinement is shown in Fig. 5. Quantitatively, the usual splitting into two contributions Nb-Nb, one short and one long arising from the edge and corner-sharing octahedron, respectively, is not strictly adopted in samples **I** and **II**. This has to be interpreted by a slight deviation in the chain local order. One notes also that the partition in the Nb-Nb population is inverted between both samples (as already suggested by the magnitude of the corresponding peaks on the FT modulus).

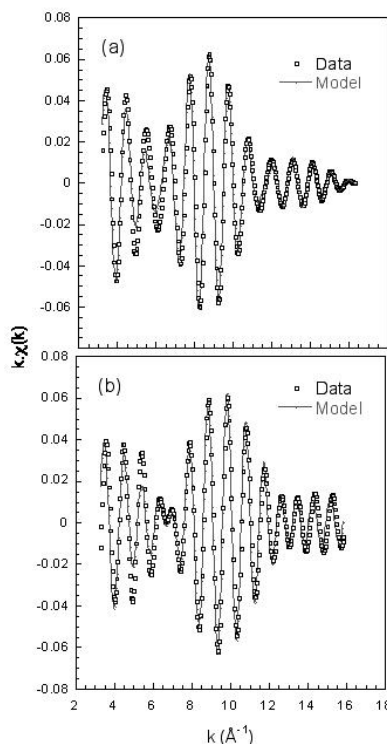


Fig. 5. Refinement of the extracted Nb-Nb EXAFS oscillations for samples (a) **I** and (b) **II**.

4. Conclusion

Slight structural modifications invisible by XRD are here evidenced by Raman spectroscopy. This is reinforced by direct observations obtained from XAS spectroscopy, and the refinement of the first cation shell (Nb-Nb backscattering) pictures an atomic arrangement closely related between both hexaniobate phases but accompanied with a slight distortion of the NbO_6 chain having for effect to inverse the corner to edge-Oh neighbours.

Acknowledgement

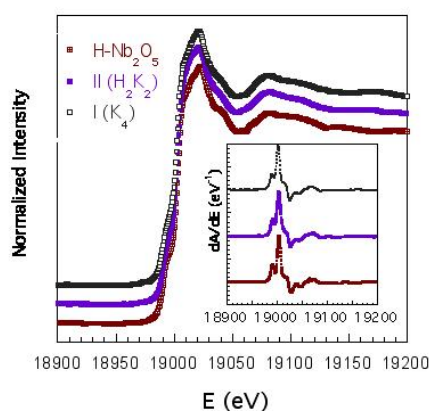
The authors would like to thank the CAPES/COFECUB through the project 557/07 and also the Brazilian agencies FAPESP and CNPq for financial support and fellowships. The authors also acknowledge LNLS (project 4337/04) for the XAS facilities.

References

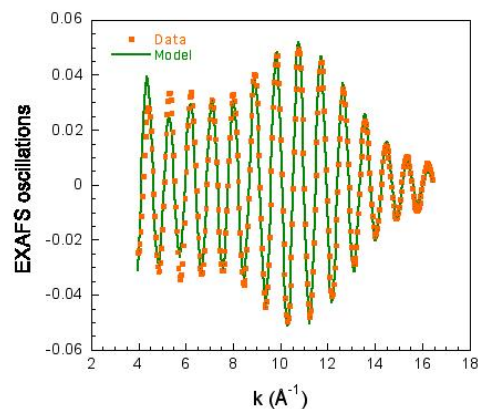
- [1] M. A. Bizeto, A. L. Shiguihara, V. R. L. Constantino, J. Mater. Chem. 19 (2009) 2512.
- [2] M. Gasperin, M. T. Bihan, J. Solid State Chem. 33 (1980) 83.
- [3] M. Gasperin, M. T. Bihan, J. Solid State Chem. 43 (1982) 346.
- [4] M. A. Bizeto, V. R. L. Constantino, Mater. Res. Bull. 39 (2004) 1729.
- [5] (a) S. W. Keller, H. N. Kim, T. E. Mallouk, J. Am. Chem. Soc. 116 (1994) 8817; (b) M. A. Bizeto, V. R. L. Constantino, Mater. Res. Bull. 39 (2004) 1811; (c) G. B. Saupe, C. C. Waraksa, H. N. Kim, Y. J. Han, D. M. Kaschak, D. M. Skinner, T. E. Mallouk, Chem. Mater. 12 (2000) 1556.
- [6] (a) U. Unal, Y. Matsumoto, N. Tamoto, M. Koinuma, M. Machida, K. Izawa, J. Solid State Chem. 179 (2006) 33; (b) S. Ida, U. Unal, K. Izawa, C. Ogata, T. Inoue, Y. Matsumoto, Mol. Cryst. Liq. Cryst. 470 (2007) 393.
- [7] A. I. Ruiz, M. Darder, P. Aranda, R. Jiménez, H. V. Damme, E. Ruiz-Hitzky, J. Nanosci. Nanotech. 6 (2006) 1602.
- [8] N. Miyamoto, K. Kuroda, J. Colloid Interface Sci. 313 (2007) 369.
- [9] M. A. Bizeto, W. A. Alves, C. A. S. Barbosa, A. M. D. C. Ferreira, V. R. L. Constantino, Inorg. Chem. 45 (2006) 6214.
- [10] A. A. Teixeira-Neto, A. L. Shiguihara, C. M. S. Izumi, M. A. Bizeto, F. Leroux, M. L. A. Temperini, V. R. L. Constantino, Dalton Trans. DOI: 10.1039/b820610d.
- [11] K. Maeda, M. Eguchi, W. J. Youngblood, T. E. Mallouk, Chem. Mater. 20 (2008) 6770.
- [12] J. M. Jehng, I. E. Wachs, Chem. Mater. 3 (1991) 100.
- [13] A. Kudo, T. Sakata, J. Phys. Chem. 100 (1996) 17323.
- [14] E. Prouzet, Chem. Mater. 15 (2003) 412.
- [15] R. Ma, K. Fukuda, T. Sasaki, M. Osada, Y. Bando, J. Phys. Chem. B 109 (2005) 6210.
- [16] K. Kato, Acta Cryst. B32 (1976) 764.
- [17] J. Liu, E. P. Kharitonova, C. G. Duan, W. N. Mei, R. W. Smith, J. R. Hardy, J. Chem. Phys. 122 (2005) 144503.
- [18] M. A. Bizeto, F. P. Christino, M. F. M. Tavares, V. R. L. Constantino, Quim. Nova 29 (2006) 1215.
- [19] M. A. Bizeto, D. L. A. De Faria, V. R. L. Constantino, J. Mater. Sc. 37 (2002) 265.
- [20] J. D. Lee, Concise Inorganic Chemistry, 5th ed., Chapman & Hall, London, 1996.

Electronic annexes (or referring procedure)

For the X-ray near edge structure (XANES) part, a Si (220) crystal monochromator scanned the energy in 2 eV-steps from 18900 to 18980 eV (accumulation time of 1 s was used per point), 0.5 eV-steps from 18980 to 19060 eV (accumulation time of 3 s), 2 eV-steps from 19060 to 19200 eV (accumulation time of 1 s), and two spectra were recorded for each sample. All energy values in Nb *K*-edge spectra were calibrated using niobium metal.



Supplementary. XANES curves at Nb *K*-edge for *H*-Nb₂O₅, and samples **I** and **II**.



Supplementary. Refinement of the extracted Nb-Nb EXAFS oscillations for $H\text{-Nb}_2\text{O}_5$ (according to crystallographic data from Table 1).

Accepted manuscript